Quantum Electronics **40** (12) 1141 – 1145 (2010)

INTERFEROMETRY

PACS numbers: 42.87.Bg; 42.79.Dj
DOI: 10.1070/QE2010v040n12ABEH013990

High-sensitive interferometric control of the quality of diffractive elements

A.M. Lyalikov

Abstract. **The prospects of the long lateral shear interferometry for controlling the quality of diffractive elements are shown. In this case, use is made of two diffractive elements, one of which is under investigation, and the other is the model one. A universal device is proposed to control the quality of the diffractive elements of both transmission and reflection types. We present the results of experimental realisation of the technique for the quality control of production of two-dimensional amplitude masks and reflection diffraction gratings.**

Keywords: *interferometer, diffractive element, long lateral shear, interference pattern, sensitivity enhancement*.

1. Introduction

Various diffractive elements made in the form of spatial periodic structures have recently found wide application in the measuring technology as optical elements [1]. Periodic structures formed on the test object in the form of measuring grids or used in various optical devices [2, 3] must meet certain metrological requirements [4]. These requirements imply the need of compliance of the groove quality of such a structure with that of a model structure.

The most accurate methods for controlling the quality of periodic structures are the interferometric method and its holographic variants [5 – 8].

Long lateral shear interferometry in the case when the value of the shear exceeds the transverse dimensions of the object under study has found practical application in the investigation of optical inhomogeneities of phase objects [9, 10]. We have considered [11 – 14] various approaches for improving the mapping sensitivity of optical inhomogeneities of phase objects for the holographic long lateral shear interferometry.

In this paper we show the prospects of the long lateral shear interferometry for controlling the quality of the diffractive elements. During this process two diffractive elements are comparatively analysed: one of the elements is controlled and the other is the model one.

A.M. Lyalikov Yanka Kupala State University of Grodno, ul. Ozheshko 22, 230023 Grodno, Belarus; e-mail: amlialikov@grsu.by

Received 21 October 2008; revision received 12 October 2010
Kvantovaya Elektronika **40** (12) 1141 – 1145 (2010)
Translated by I.A. Ulitkin

2. Interferometric control device

Figure 1 shows the optical scheme of a device allowing one to carry out interferometric quality control of diffractive elements of transmission and reflection types.

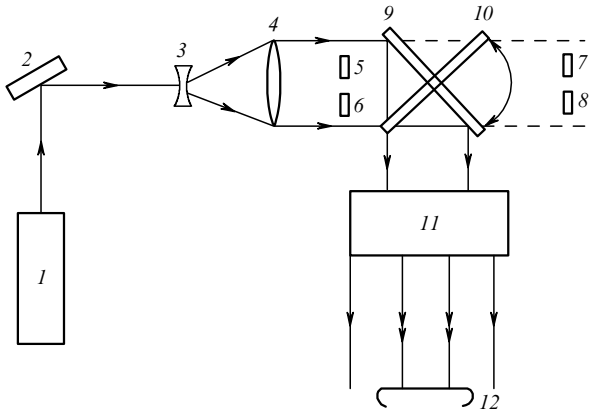

Figure 1. Optical scheme of the device for the interferometric quality control of the diffractive elements: (*1*) laser light source; (*2*) mirror; (*3, 4*) telescopic system; (*5, 6*) and (*7, 8*) model and controlled diffractive elements of transmission and reflection types, respectively; (*9, 10*) positions of the semitransparent mirrors in the regimes of the quality control of transmission and reflection elements, respectively; (*11*) lateral shear interferometer; (*12*) plane of the interference pattern.

The collimated probe light beam is formed by a laser light source (*1*), mirror (*2*), and telescopic system (*3, 4*). It should be noted that high requirements are imposed on the quality of optical elements of the telescopic system forming a planar wavefront. Due to the fact that the model and controlled diffractive elements of both transmission and reflection types [(*5, 6*) and (*7, 8*), respectively] are located in different parts of the probe beam wavefront, the radiation light source (*1*) should have a high degree of spatial coherence to obtain high quality interference patterns. For interferometric control, we used the LGN-212 helium – neon laser, which emits at a wavelength of 633 nm.

By rotating the semitransparent mirror, a part of the probe beam is used for the quality control of transmission [position (*9*)] and reflection [position (*10*)] diffractive elements. In the first case, the probe light beam [after passing through the model and controlled elements (*5*) and (*6*)] is directed by the semitransparent mirror (*9*) to the interferometer (*11*), which implements a long lateral shift, exceeding the linear dimensions of the optical elements.

As a long lateral shear interferometer we used in the experiments a compact interferometer [8, 9] based on four mirrors (Fig. 2). The interferometer had an optical spatial filtering system, traditionally [15] in the form of two objectives (*7, 9*) and aperture (*8*) with a pinhole. This system was designed to extract, from the whole set of light beams diffracted by the model and the controlled elements in different diffraction orders, only two beams diffracted by these elements in the same order. The telescopic system (*1, 2*) located at the interferometer input was used to reduce the beam diameter.

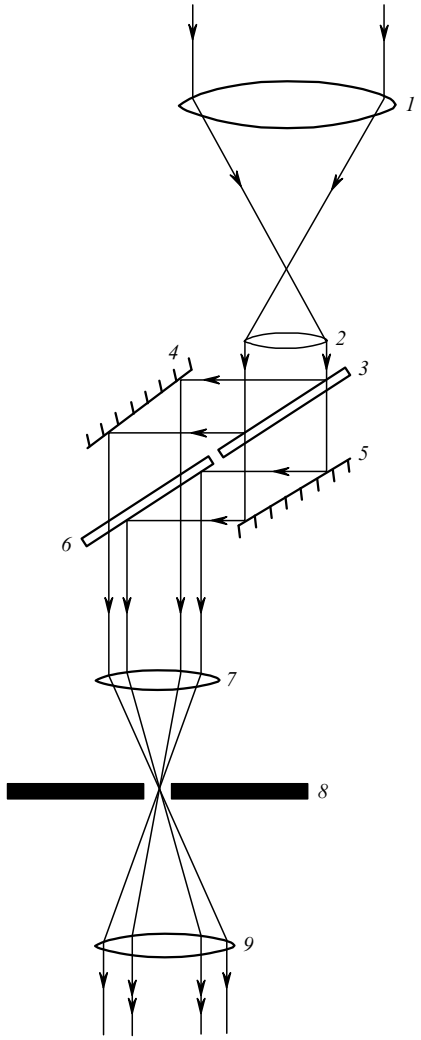

Figure 2. Scheme of the lateral shear interferometer: (*1, 2*) objectives of the telescopic system; (*3–6*) interferometer mirrors; (*7, 9*) objectives of the optical spatial filtering system; (*8*) aperture with a pinhole.

When controlling the quality of the reflection diffractive elements, the probe light beam passes through the semitransparent mirror (Fig. 1) and diffracts by the model and the controlled elements (*7*) and (*8*). The diffracted beams are directed into the interferometer (*11*) by the semitransparent mirror (*10*).

3. Method of the interferometric control

When implementing the technique of the interferometric control, the model (M) and controlled (C) diffractive elements (*5*) and (*6*) or (*7*) and (*8*) (Fig. 1) of transmission or reflection types, respectively, are placed in different halves of the cross sections (zones 1 and 2) of the probe light beam, as shown in Fig. 3a. Let us match the coordinate system xy with the planes of the model and controlled diffractive elements (Fig. 3a). We assume that the optical system forms the object wave with a plane wavefront. In this case, the aberrations of the optical control system can be neglected. If this condition cannot be fulfilled, we should take into account the systematic error component arising from wavefront aberrations to ensure the control reliability.

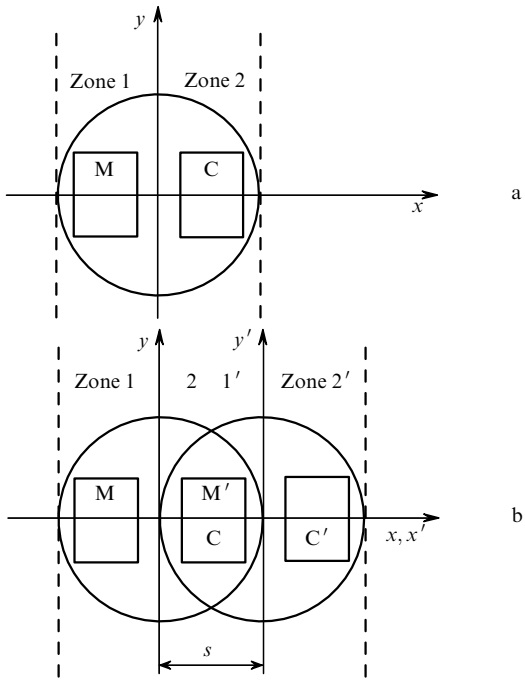

Figure 3. Schematics of the light beam cross section (circle) as well as of the model (M) and controlled (C) diffractive elements (rectangles), after the light beam passes through these elements (a) and the first and second interfering light beams shifted in space by s are superimposed in the plane of the interference pattern formation (b).

To simplify the description of the technique, we assume that the projections of the grooves of the periodic structures of the diffractive elements on the xy plane are oriented parallel to the x axis. We present the expressions for the amplitude transmission (or reflection) coefficients of the controlled and model diffractive elements in the form

$$\tau_{\mathrm{m,c}}(x,y) = \sum_{n=-\infty}^{+\infty} a_n \exp\left[\frac{2\pi n y}{P} + n\varphi_{\mathrm{m,c}}(x,y)\right], \qquad (1)$$

where the parameters with the subscript 'm' refer to the model element, and with the subscript 'c' – to a controlled one; a_n are the coefficients; n is the diffraction order; P is the average period of the projection of the structures on the xy plane; $\varphi_{\mathrm{m,c}}(x,y)$ are the functions that determine the deviation of the periods of the projections of the structures of controlled and model elements from the average period P. It is obvious that the difference between the functions $\varphi_{\mathrm{m}}(x,y)$ and $\varphi_{\mathrm{c}}(x,y)$ can be used to estimate the deviation

of the parameters of the periodic structure of the controlled element from the parameters of the model element.

The probe beam (after passing through diffractive elements or after reflecting from these elements) is a set of diffracted elements which propagate at different angles to the optical axis of the device, the angles being determined by the spatial frequencies of the beams η_n. The expression for the phase $\Phi_n(x, y)$ of any light wave can be conveniently represented in the form of separate expressions for each of the zones (zone numbers are indicated in Fig. 3a):

$$\Phi_n(x,y) = \begin{cases} 2\pi\eta_n y + n\varphi_{\mathrm{m}}(x,y) & \text{for zone 1,} \\ 2\pi\eta_n y + n\varphi_{\mathrm{c}}(x,y) & \text{for zone 2,} \end{cases} \tag{2}$$

where $\eta_n = \cos\alpha_n/\lambda$; α_n is the angle between the propagation direction of the beam diffracted to the nth order and the axis y; λ is the wavelength.

Consider the peculiarities of the interference pattern formation. For the first light beam extracted by the optical spatial filtering system in the interferometer (*11*) (Fig. 1), we will use the same coordinate system xy and designations of optical elements as in Fig. 3a. For the second beam extracted by the optical spatial filtering system, we will introduce the coordinate system $x'y'$ and denote the model and controlled diffractive elements by M′ and C′, respectively. We assume that the first light beam propagates strictly along the optical axis of the device and the second – at some small angle to the axis of the first beam. The expressions for the complex amplitudes of the light waves, generated in the interferometer and extracted by optical spatial filtering system, can be represented, in this case, in the coordinate systems xy and $x'y'$:

$$A(x,y) \propto \begin{cases} 1 + \exp\{\mathrm{i}[\varphi_{\mathrm{m}}(x,y)]\} & \text{for zone 1,} \\ 1 + \exp\{\mathrm{i}[\varphi_{\mathrm{c}}(x,y)]\} & \text{for zone 2,} \end{cases} \tag{3}$$

$$A'(x',y') \propto \begin{cases} 1 + \exp\{\mathrm{i}[(2\pi/\lambda)(x'\cos\alpha + y'\cos\beta) \\ \quad + \varphi_{\mathrm{m}}(x',y')]\} & \text{for zone } 1', \\ 1 + \exp\{\mathrm{i}[(2\pi/\lambda)(x'\cos\alpha + y'\cos\beta) \\ \quad + \varphi_{\mathrm{c}}(x',y')]\} & \text{for zone } 2', \end{cases} \tag{4}$$

where α and β are the angles between the propagation directions of the second light beam and the axes x' and y', respectively. The expression for the complex amplitude of the second light wave (4) in the coordinate system xy can be written in the form

$$A'(x,y) \propto \begin{cases} 1 + \exp\{\mathrm{i}[(2\pi/\lambda)(x\cos\alpha + y\cos\beta) \\ \quad + \varphi_{\mathrm{m}}(x-s,y)]\} & \text{for zone } 1', \\ 1 + \exp\{\mathrm{i}[(2\pi/\lambda)(x\cos\alpha + y\cos\beta) \\ \quad + \varphi_{\mathrm{c}}(x-s,y)]\} & \text{for zone } 2'. \end{cases} \tag{5}$$

When controlling the quality of the elements, the value of the lateral shear s is chosen equal to the distance between the centres of the model (M) and controlled (C) diffractive elements (Fig. 3b). In other words, the shear s must be such that in the observation plane (*12*) (Fig. 1) of the interference pattern, the images of the controlled element C formed by the first light beam are superimposed with the images of the model element M′ formed by the second beam (Fig. 3b). Thus, in the plane (*12*) two light waves, described by the expressions (3) and (5), are superimposed to form an interference pattern in the superimposed zones 2 and 1′ for the first and second light beams, respectively. The light intensity distribution $I(x, y)$ in the interference pattern in the plane (*12*) is described by the expression

$$I(x,y) = [A(x,y) + A'(x,y)][A^*(x,y) + A'^*(x,y)]. \tag{6}$$

Taking into account the interference pattern formation only in the superimposed zones 2 and 1′, we obtain, in view of expressions (3), (5), and (6), the intensity distribution

$$I(x,y) \sim 1 + \cos[2\pi(\xi x + \eta y) + \delta\varphi], \tag{7}$$

where $\xi = \cos\alpha$ and $\eta = \cos\beta/\lambda$ are the parameters characterising the width and orientation of the interference fringes that are determined according to (5) by the propagation direction of the second light beam; $\delta\varphi = |\varphi_{\mathrm{m}}(x,y) - \varphi_{\mathrm{c}}(x,y)|$. Distribution (7) characterises the differences of the controlled diffraction element from the model one, the differences being governed by the phase distribution $\delta\varphi$.

To improve the control reliability, it is desirable to obtain several interference patterns with various fringe adjustments defined by the parameters ξ and η. Obtaining the interference pattern in the fringes of infinite width corresponds to $\xi = 0$ and $\eta = 0$. To adjust the interference fringes horizontally, the condition $\xi = 0$ should be met, and vertically – the condition $\eta = 0$. The fringe widths P_y and P_x for the last two special cases will be determined by the parameters η and ξ, respectively, i.e., $P_y = \lambda/\cos\beta$ and $P_x = \lambda/\cos\alpha$.

We noted above that in obtaining the interference pattern in the plane (*12*) (Fig. 1), the images of the controlled element C and model element M′ (Fig. 3b) formed by the first light beam and second light beams, respectively, should be exactly superimposed. The acceptable inaccuracy in superimposition of the images of the elements C and M′ in the plane xy can be found from the condition under which this shear leads to a bend of the interference fringe by a value of no more than 0.1 period.

4. Experimental realisation of the control method

The above method of the interferometric control was tested for diffractive elements of transmission and reflection types.

We controlled the quality of the amplitude masks representing a two-dimensional periodic structure in the form of 40-μm-thick stretched thin threads, arranged crosswise. These diffractive elements were used as measuring grids, intended for studying phase objects by the defocused grid method [16], as well as to visualise the surface shape by the fringe projection method [17]. Fabrication of metal diffraction gratings made it possible to use high-power radiation sources in measuring systems.

The average period of the structures was 165 μm. To ensure the high quality of the amplitude mask required the control of the compliance of the structure period with the model amplitude mask period. Figure 4 shows the diffraction spectrum of a cross grating, observed in the back focal plane of the objective, when the grating is illuminated by coherent light. The interferometric control device is configured to operate in the regime of the quality control of the transmission diffractive elements, i.e., the semitransparent mirror is set to position (*9*) (Fig. 1). The model and

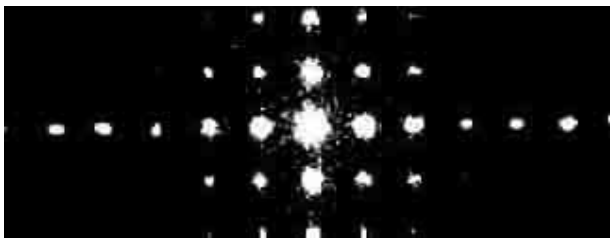

Figure 4. Diffraction spectrum of the controlled two-dimensional transmission diffraction grating.

controlled amplitude masks measured 140 × 110 mm in size. Figure 5 shows the interference patterns in the fringes of finite width, reflecting the difference between the behaviour of the functions $\varphi_m(x, y) - \varphi_c(x, y)$ for the diffraction grating formed by the vertical threads.

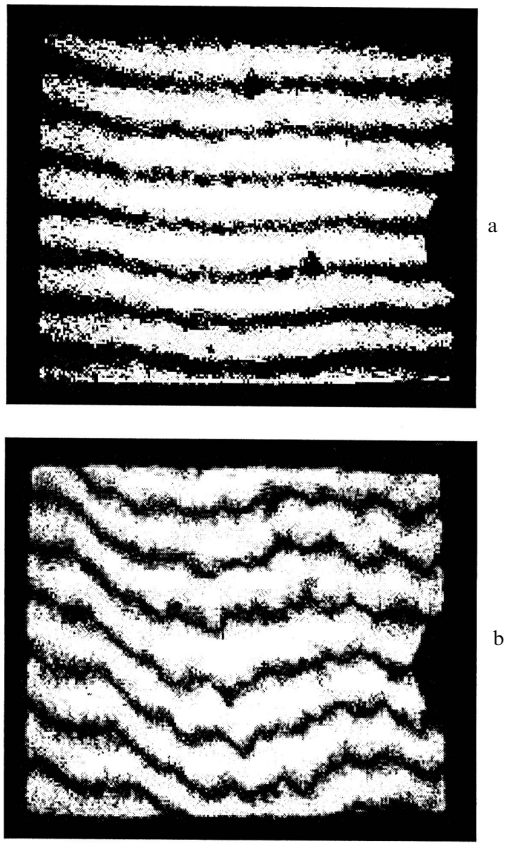

Figure 5. Interference patterns showing (with different sensitivities) the differences between the controlled and model gratings. The patterns were obtained by extracting +1st (a) and +3rd (b) diffraction orders by the optical spatial filtering system.

The first interference pattern (Fig. 5) was obtained as described above: the optical spatial filtering system extracted +1st diffraction orders. The second interference pattern was obtained by extracting +3rd diffraction orders (Fig. 5b) placed on a horizontal line in the spectrum of the diffraction grating (Fig. 4). The sensitivity of the difference mapping $\varphi_m(x, y) - \varphi_c(x, y)$ in the latter case is increased by three times, which is evidenced by a large bend in proportion to the interference fringes in the central zone of the superimposed image masks. The second interferogram makes it possible to determine more accurately the difference in the arrangement of the threads in the structure from their location in the model structure. For example, it follows from the interference patterns that in some areas of the central zone of the amplitude mask under study this difference is about 80 μm.

We also controlled the quality of the reflection diffraction gratings, which form a system of spatially divergent light beams in the device. In addition to the equalisation of the diffraction efficiency of diffraction orders, the given diffractive element should ensure the formation of the wavefront of a particular shape. Figure 6 shows the results of the interferometric control of the reflection diffraction grating quality by using the procedure described above. We used +4th diffraction order to obtain the interference patterns. We obtained the interference patterns with different fringe adjustments, which confirms the need to increase the sensitivity in the process, especially when visualising small differences between the controlled element and the model one. We failed to visualise on the interference pattern in the fringes of infinite width any differences in the shapes of the wavefronts formed in +4th diffraction orders by the controlled and model elements (Fig. 6a). If the fringes were adjusted successfully, in this case these are fringes of finite width located horizontally, we managed to observe a slight defect in the lower part of the controlled diffractive element, which manifests itself as the curvature of the fringe (Fig. 6b). This curvature corresponds to the deviation of the wavefront of the beam diffracted in the +4th order from

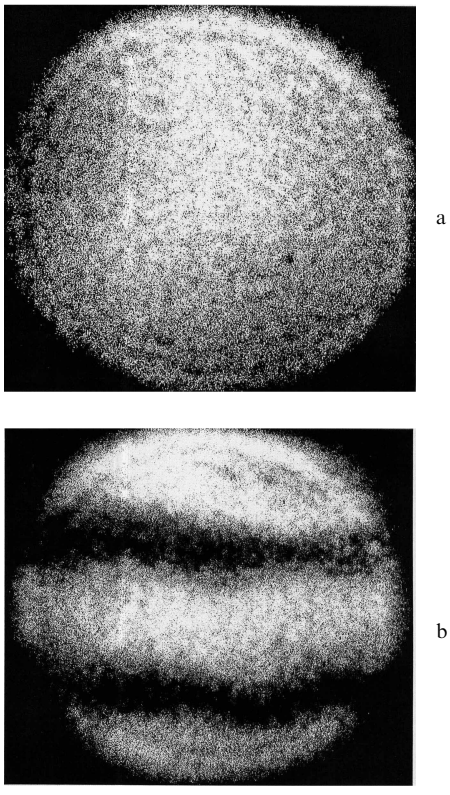

Figure 6. Interference patterns showing the deviation of the wavefront formed in the +4th order by the controlled diffraction grating from the front formed in the same order by the model grating. The patterns were obtained in the fringes of infinite (a) and finite (b) width.

the model wavefront of the beam diffracted in the same order at $\sim 0.1\lambda$. It should be noted that in the interferometric control of the quality of the diffractive element with the lower diffraction orders, this defects cannot be observed.

5. Conclusions

Thus, the developed technique and universal device for the interferometric control of the diffractive element quality allow relatively simple implementation of the quality control of elements of transmission and reflection types and can be used in the manufacturing environment. This technique can also be successfully applied for the certification of diffractive elements.

References

1. Poleshchuk A.G., Koronkevich V.P., Korolkov V.P., Sedukhina A.G. *Komputer. Opt.*, **22**, 86 (2002).
2. Shi Ling, Grunder K.P., Klingelhoffer H. *Meas. Sci. Technol.*, **9**, 739 (1998).
3. Fattakhov Ya.V., Galyautdinov M.F., L'vova T.N. *Opt. Spektrosk.*, **89**, 150 (2000).
4. Dich Z.L. *Opt. Spektrosk.*, **83**, 509 (1997).
5. Malacara D. (Ed.) *Optical Shop Testing* (New York: Wiley, 1978).
6. Lyalikov A.M. *Opt. Spektrosk.*, **92**, 344 (2002).
7. Lyalikov A.M. *Opt. Spektrosk.*, **93**, 875 (2002).
8. Lyalikov A.M. *Opt. Spektrosk.*, **98**, 522 (2005).
9. Komissarchuk V.A., in *Issledovanie prostranstvennykh gazodinamicheskikh techenii na osnove opticheskikh metodov. Trudy VVIA im. N.E. Zhukovskogo* (The Study of Spatial Gas-Dynamic Flows by Optical Methods. Proceedings of the N.E. Zhukovsky All-Union Higher Engineering Academy) (Moscow: 1971) p. 121.
10. Beketova A.K., Belozerov A.F., Berezkin A.N., et al. *Golograficheskaya interferometriya fazovykh ob'ektov* (Holographic Interferometry of Phase Objects) (Leningrad: Nauka, 1979).
11. Lyalikov A.M. *Kvantovaya Elektron.*, **35**, 290 (2005) [*Quantum Electron.*, **35**, 290 (2005)].
12. Lyalikov A.M. *Opt. Spektrosk.*, **99**, 151 (2005).
13. Lyalikov A.M. *Opt. Spektrosk.*, **102**, 874 (2007).
14. Lyalikov A.M. *Opt. Spektrosk.*, **105**, 136 (2008).
15. Goodman J. *Introduction to Fourier Optics* (New York: McGraw-Hill, 1996).
16. Vasiliev L.A. *Schlieren Methods* (New York: Israel Program for Scientific Translations,1971).
17. Vest C.M. *Holographic Interferometry* (New York: Wiley, 1979).